

# A neuron-specific cytoplasmic dynein isoform preferentially transports TrkB signaling endosomes

Junghoon Ha,<sup>1</sup> Kevin W.-H. Lo,<sup>1</sup> Kenneth R. Myers,<sup>1</sup> Tiffany M. Carr,<sup>1</sup> Michael K. Humsi,<sup>1</sup> Bareza A. Rasoul,<sup>1</sup> Rosalind A. Segal,<sup>2,3</sup> and K. Kevin Pfister<sup>1</sup>

<sup>1</sup>Department of Cell Biology, School of Medicine, University of Virginia, Charlottesville, VA 22908

<sup>2</sup>Department of Neurobiology and <sup>3</sup>Department of Pediatric Oncology, Dana-Farber Cancer Institute, Harvard Medical School, Harvard University, Boston, MA 02115

Cytoplasmic dynein is the multisubunit motor protein for retrograde movement of diverse cargoes to microtubule minus ends. Here, we investigate the function of dynein variants, defined by different intermediate chain (IC) isoforms, by expressing fluorescent ICs in neuronal cells. Green fluorescent protein (GFP)-IC incorporates into functional dynein complexes that copurify with membranous organelles. In living PC12 cell neurites, GFP-dynein puncta travel in both the anterograde and retrograde directions. In cultured hippocampal neurons,

neurotrophin receptor tyrosine kinase B (TrkB) signaling endosomes are transported by cytoplasmic dynein containing the neuron-specific IC-1B isoform and not by dynein containing the ubiquitous IC-2C isoform. Similarly, organelles containing TrkB isolated from brain by immunoprecipitation also contain dynein with IC-1 but not IC-2 isoforms. These data demonstrate that the IC isoforms define dynein populations that are selectively recruited to transport distinct cargoes.

## Introduction

Cytoplasmic dynein, the microtubule minus end-directed motor protein, is essential for many cellular functions including organelle trafficking, mitosis, virus transport, and cell migration (Vallee et al., 2004; Levy and Holzbaur, 2006). In neurons, dynein is responsible for the fast retrograde transport of membrane-bound organelles, such as signaling endosomes, from the axon terminus to the cell body. Signaling endosomes are formed when neurotrophins, which are target-derived growth factors such as NGF and brain-derived neurotrophic factor, bind to and activate their individual tyrosine kinase receptors (Trks), TrkA and TrkB, respectively (Bhattacharyya et al., 2002; Delcroix et al., 2003; Huang and Reichardt, 2003; Ye et al., 2003; Heerssen et al., 2004). Retrograde transport of signaling endosomes from axon terminals to cell bodies is required for neuronal survival and axonal plasticity.

Very little is known about how cytoplasmic dynein is regulated to accomplish its varied functions. A single gene encodes the dynein motor domain, the >500-kD heavy chain (Pfister et al., 2006). However, at least two genes encode each of the five subunits that make up the cargo-binding domain: the intermedi-

ate chain (IC; DYNC11), the light IC, and three classes of light chains. Cells thus contain distinct dynein complexes distinguished by different combinations of subunit isoforms, and it is hypothesized that these distinct dynein complexes make possible specific regulation of dynein motor activity and/or cargo binding (Tai et al., 1999; Tynan et al., 2000; Susalka and Pfister, 2000; Pfister et al., 2006; Lo et al., 2007a; O'Rourke et al., 2007). There is evidence that dynein complexes with different IC isoforms have distinct roles in cells. At least six IC isoforms are generated by alternative splicing. IC-2C (the product of gene 2, alternative splicing variant C) is the only ubiquitously expressed isoform. Several of the IC isoforms are expressed exclusively in neurons, and the levels of the isoforms are regulated during brain development (Pfister et al., 1996a,b; Myers et al., 2007). In addition, dynein complexes containing distinct IC and light IC isoforms are segregated in adult rat optic nerve axons (Dillman et al., 1996).

To identify functional differences between dynein complexes containing different ICs, we imaged two fluorescently tagged IC isoforms in living neuronal cells. We found that the fluorescent ICs incorporated into functional dynein complexes that bound to microtubules and membranous organelles. Analysis of the movement of dynein complexes containing the ubiquitous isoform IC-2C and a neuron-specific isoform IC-1B (gene 1, alternative splicing variant B) revealed differences in

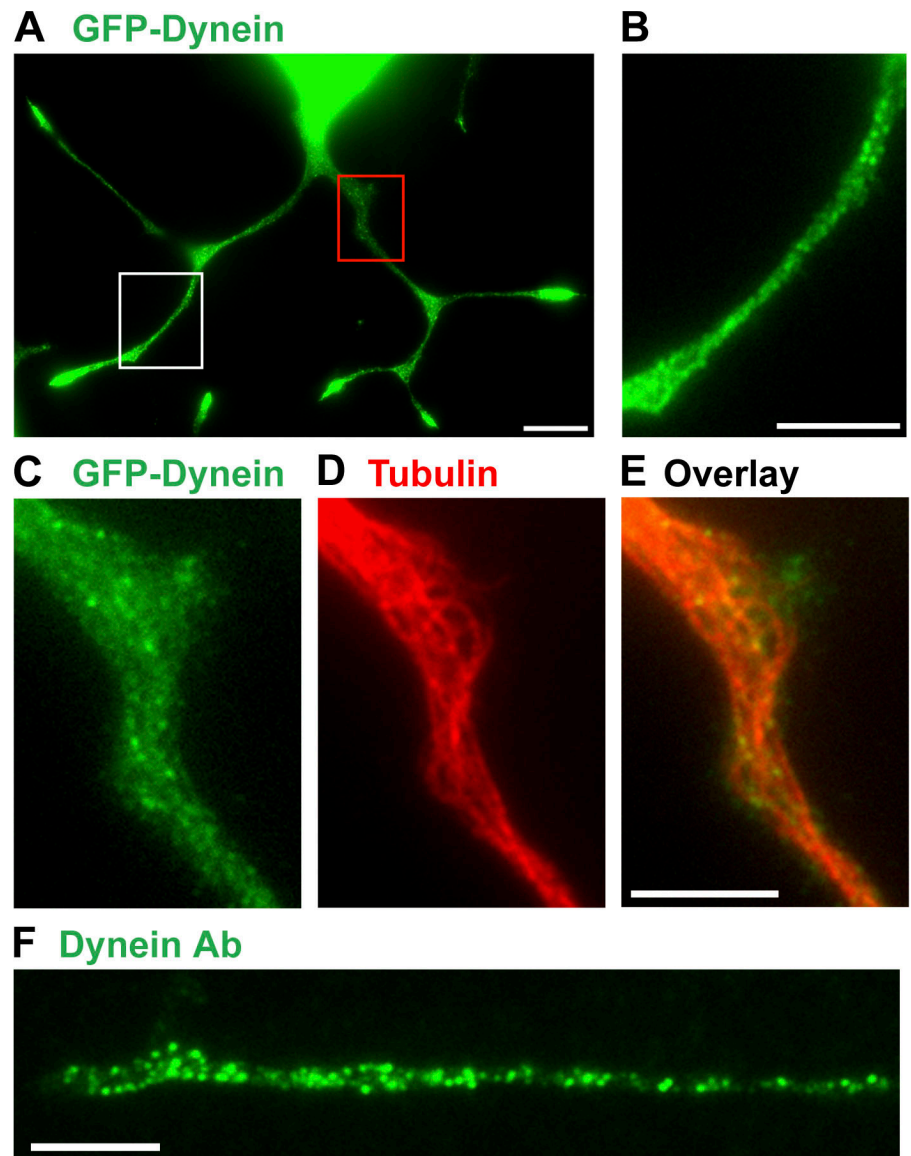
J. Ha and K.W.-H. Lo contributed equally to this paper.

Correspondence to K. Kevin Pfister: kkp9w@virginia.edu

Abbreviations used in this paper: IC, intermediate chain; mRFP, monomeric red fluorescent protein; Trk, neurotrophin tyrosine receptor kinase.

The online version of this paper contains supplemental material.

**Figure 1. Localization of GFP-dynein puncta near microtubules in PC12 cell neurites.** (A–E) PC12 cells with stable expression of GFP–IC-2C (GFP–Dynein, green) were differentiated with NGF, fixed, and stained with anti-tubulin (red). (A, B, C, and E) GFP-dynein; (D and E) tubulin. (A) PC12 cell with multiple neurites. (B) Enlargement of a region containing discrete dynein puncta indicated by the white box in A. (C–E) Enlargements of the GFP, tubulin, and overlay images, respectively, of the region indicated by the red box in A. (F) Neurite of an untransfected PC12 cell stained with pan dynein antibody 74.1 (Dynein Ab, green). Bars: (A) 10  $\mu$ m; (B–F) 5  $\mu$ m.



their kinetic properties. In addition, the dynein complexes containing the IC-1B isoform but not the IC-2C isoform bound to and transported neuronal TrkB signaling endosomes. In PC12 cells, however, dynein containing IC-2C copurified with TrkA signaling endosomes. In this cell line, NGF binding to TrkA lead to an increase in the amount of activated TrkA that copurified with dynein-associated membrane-bounded organelles and increased retrograde dynein velocity but had no effect on anterograde dynein velocity in neurites. These data indicate that different IC isoforms contribute to the regulation of dynein cargo binding.

## Results

We generated a stable PC12 cell line expressing low levels (<15% of the total) of GFP-tagged IC isoform 2C (GFP–IC-2C) and used it to characterize the properties of dynein complexes containing the IC-2C isoform. In cell bodies, few discrete GFP–IC-containing structures were resolved due to the presence of a

large soluble dynein pool (Paschal et al., 1987; Habermann et al., 2001). However, in neurites, the distribution of GFP–dynein was punctate and comparable to that observed with an antibody to dynein (Fig. 1). Some regions of the neurites were wide enough to distinguish microtubules, and in these regions, the GFP–dynein puncta colocalized with the microtubules (Fig. 1).

Fig. 2 A shows that most of the endogenous dynein IC, and the GFP–IC, copelleted with microtubules. This indicated that the GFP–IC, like the endogenous IC, was bound to the microtubule-binding motor domain of the dynein complex, the heavy chain. In addition, dynein containing the GFP–IC was released from microtubules in the presence of Mg-ATP, demonstrating that the GFP–IC containing dynein hydrolyzed ATP. Fig. 2 B shows that after sucrose density gradient sedimentation, all of the GFP–IC-2C, like the endogenous IC, copurified exclusively with 20S dynein complexes near the bottom of the gradient (Fig. 2 B). The absence of GFP–IC at the top of the gradient showed that there was no free pool of GFP–IC. Therefore all the GFP–IC-2C incorporated into

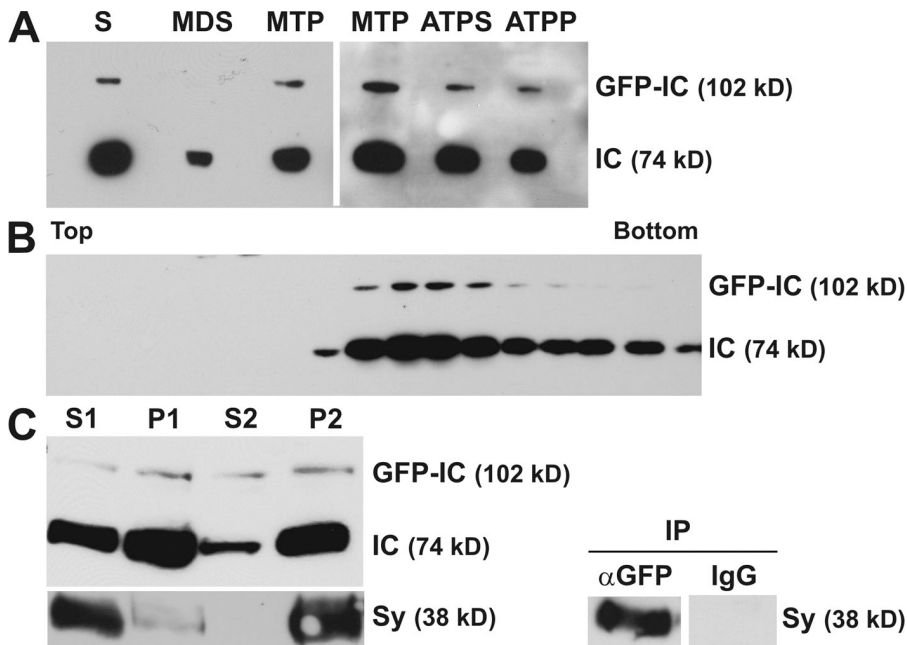


**Figure 2. Biochemical characterization of the incorporation of the GFP-IC-2C isoform into functional cytoplasmic dynein complexes.** (A) Microtubule binding. Western blots of the indicated fractions prepared from PC12 cells with stable expression of GFP-IC-2C were probed with a pan antibody to dynein ICs (74.1) that recognized both the endogenous IC (IC) and GFP-tagged IC (GFP-IC). Taxol-stabilized microtubules were added to the soluble fraction (S), and centrifugation yielded the microtubule depleted supernatant (MDS) and microtubule pellet (MTP). The microtubule pellet was resuspended in 10 mM Mg-ATP, and centrifugation yielded the ATP supernatant (ATPS) and microtubule pellet (ATPP). The identity of the GFP-IC-2C bands was confirmed with an antibody to GFP (not depicted). Densitometry was used to estimate that the GFP-IC pool was <15% of the total IC pool. (B) Sucrose density gradient sedimentation. The soluble fraction was also fractionated by sucrose density gradient centrifugation, and the proteins in the fractions were analyzed by SDS-PAGE and Western blotting. The blot was probed with the pan dynein antibody. The fractions at the top (5% sucrose) and bottom (20% sucrose) of the gradient are indicated above the blot. (C) Association with

membrane-bounded organelles. PC12 cells were lysed in a cytoplasm-like buffer and fractionated; the postnuclear supernatant (S1) and pellet (P1), high-speed supernatant (S2), and high-speed membrane fraction (P2) are indicated. Immunoprecipitation (IP): magnetic beads, preloaded with antibodies to GFP ( $\alpha$ GFP) or control IgG (IgG), were incubated with the membrane fraction, P2. The beads were washed and the fractions were analyzed by SDS-PAGE, and the Western blots were probed with the pan dynein antibody and an antibody to synaptophysin (SY), a membranous organelle marker.

functional dynein complexes, and the GFP-IC puncta observed in cells corresponded to these complexes. In addition, two membrane vesicle markers, synaptophysin and the transmembrane neurotrophin receptor TrkA, were purified by immunaffinity chromatography from a membrane fraction by antibodies to GFP coupled to magnetic beads (Fig. 2 C and see Fig. 8 C). This result established that dynein containing the GFP-IC associated with membranous organelles.

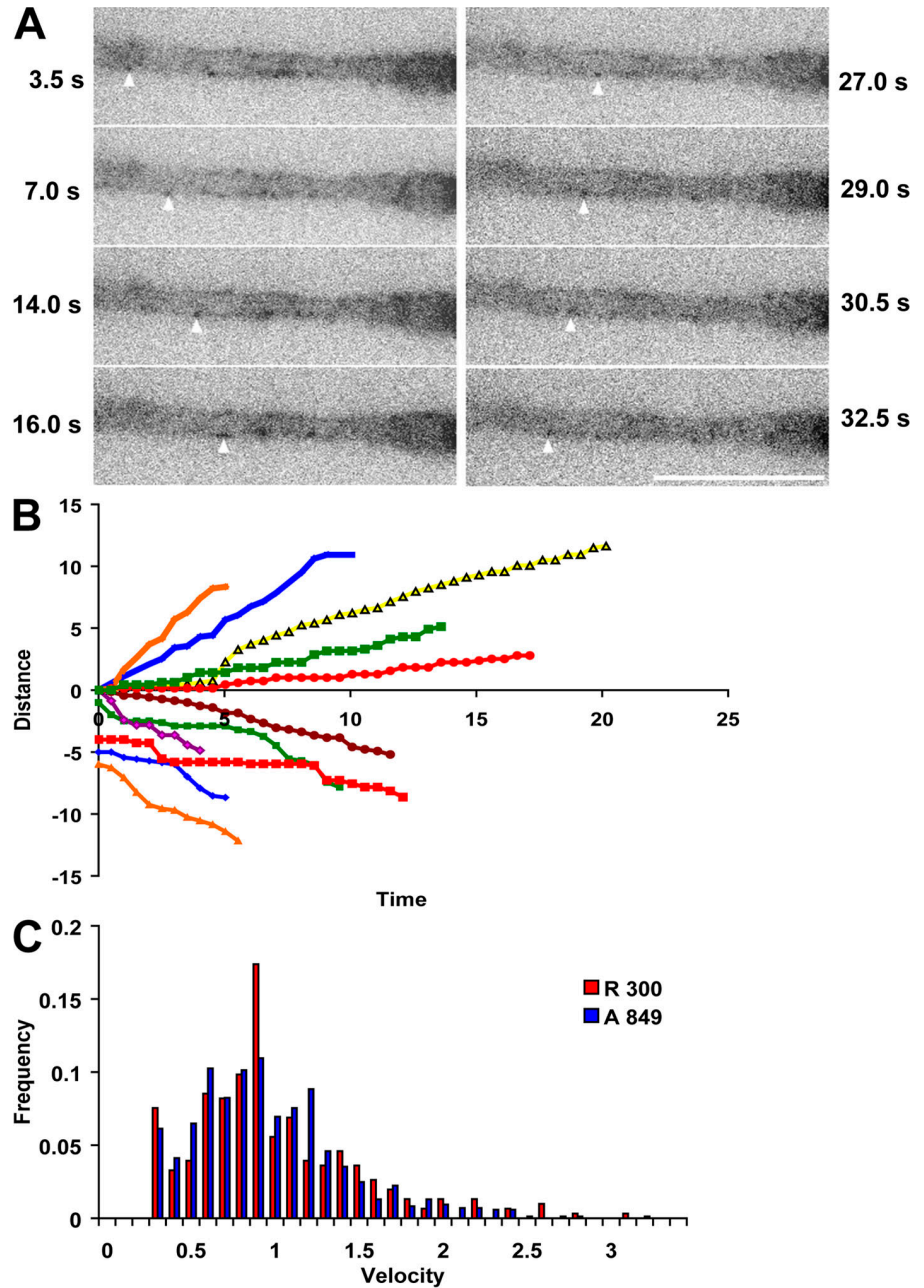
In living PC12 cell neurites, GFP-IC-2C dynein puncta were observed to move rapidly along linear tracks in both the anterograde (toward the tip) and retrograde (toward the cell body) directions (Fig. 3 A and Video 1, available at <http://www.jcb.org/cgi/content/full/jcb.200803150/DC1>). We found that 92% of the growing microtubules ( $n = 53$ ) in PC12 cells were oriented with their plus ends toward the tip by use of the EB3 polarity assay. Therefore, as in axons, anterograde movement in PC12 cell neurites is directed toward microtubule plus ends, and retrograde movement is directed toward microtubule minus ends. Frame-to-frame tracking of the movement of individual dynein puncta showed that their velocity changed during excursions (see Materials and methods; Fig. 3 B). The interval velocities of the puncta were in the range of 0.3–3.1  $\mu$ m/s, and the mean interval velocity for retrograde dynein movement was 0.9  $\mu$ m/s (Fig. 3 C and Table I). A larger number of the dynein puncta were observed moving in the anterograde direction than the retrograde direction in the PC12 cell neurites. This was consistent with the observation that dynein accumulated in growth cones (Fig. 1 A; Myers et al., 2007). To further demonstrate that the retrograde motility of GFP-IC dynein complexes was the result of their motor activity, siRNA specific for the untranslated region of IC-2 gene products was

used to deplete the endogenous dynein pool while allowing expression of the GFP-tagged IC (Fig. 4). Robust GFP-dynein puncta movement in PC12 cell neurites continued after the depletion of the endogenous IC-2 isoforms, which would normally cause the cessation of movement (Fig. 4 and Video 2). This observation confirmed that the GFP-dynein complexes moving in the retrograde direction were active motors, rather than cargo of the endogenous dynein.

To identify differences in the functional roles of the dynein complexes with distinct ICs in neurons, we used live cell imaging of fluorescent dynein IC isoforms transfected into cultured hippocampal neurons. The kinetic and cargo-binding properties of dynein complexes with two isoforms, the ubiquitous isoform IC-2C and the neuron-specific isoform IC-1B, were determined. In the axons of hippocampal neurons, dynein complexes containing IC-2C and IC-1B moved rapidly in both the anterograde and retrograde directions (Fig. 5, A and B; and Videos 3 and 4, available at <http://www.jcb.org/cgi/content/full/jcb.200803150/DC1>). In contrast to the movement of IC-2C-containing dynein complexes in PC12 cell neurites, no directional bias for either of the two distinct dynein complexes was observed in hippocampal neuron axons. Significantly more of the dynein complexes containing IC-2C were found to be nonmotile than the dynein complexes containing IC-1B ( $P < 0.0005$ ; Table II). Large numbers of both classes of dynein complexes displayed jiggling motion but no net motility. Occasionally, the jiggling movement was observed to precede or follow a motile excursion. There was no significant difference between the retrograde interval velocity distributions of the two classes of dynein (Fig. 6). The range of velocities observed for dynein complexes with either IC-2C

Figure 3. **Bidirectional movement of dynein complexes containing IC-2C in a PC12 cell neurite.**

(A) Live cell imaging. Individual frames from a video (Video 1, available at <http://www.jcb.org/cgi/content/full/jcb.200803150/DC1>) of GFP-IC-2C dynein puncta moving in a PC12 cell neurite. (left) Arrowheads indicate GFP-IC-2C dynein puncta moving in the anterograde direction. (right) Arrowheads indicate GFP-IC-2C dynein puncta moving in the retrograde direction. The time from the start of the video is indicated to the right and left of the panels. Bar, 10  $\mu\text{m}$ . (B) Displacement tracking of IC-2C dynein excursions in PC12 cell neurites. The positions of representative individual dynein puncta were tracked along the neurite in each frame of the videos, and the linear displacements (in micrometers) of 11 individual dynein puncta are graphed against time (in seconds) of movement. Anterograde movement is recorded as positive displacement and retrograde movement as negative. The initial positions of the puncta were set to 0, whereas the displacements of some of the retrogradely moving puncta were offset on the y axis to distinguish them on the graph. (C) Interval velocity distribution of dynein containing IC-2C in neurites of the stable PC12 cell line. Velocities ( $\mu\text{m}/\text{s}$ ) of individual movements of GFP-IC-2C dynein puncta between two frames were plotted against the frequency of their occurrence; motility in the anterograde direction (blue) or retrograde direction (red) is indicated. (inset) The number of measurements for the anterograde (A) and retrograde (R) directions.



or IC-1B was 0.3–3.6  $\mu\text{m}/\text{s}$  in hippocampal axons. However, compared with PC12 cells, a larger number of slow velocities were observed in axons. This accounts for the net slower mean interval velocities (0.7  $\mu\text{m}/\text{s}$ ) calculated for both dynein isoforms. The kinetics of dynein excursions in the retrograde direction were also analyzed. There was no significant difference in either the mean excursion velocities or run lengths when dynein complexes containing IC-2C and IC-1B were compared. However, on average, the excursions of dynein containing IC-1B lasted  $\sim 30\%$  longer ( $P < 0.0003$ ). Some puncta from both classes of dynein were observed to switch direction during excursive movement in hippocampal axons. Interestingly, a dynein puncta was as likely to switch from the retrograde to the anterograde direction as the anterograde to retrograde direction (unpublished data). No significant dif-

ference was observed between the anterograde interval velocity distributions of dynein complexes with IC-1B and IC-2C in axons (Table III and not depicted). However, the mean anterograde excursion velocity of dynein with IC-2C was slightly faster than that of dynein with IC-1B ( $P < 0.02$ ).

We also characterized the binding of dynein complexes with different ICs to one cargo, TrkB signaling endosomes. In neurons, the retrograde transport of signaling endosomes (which contain activated, neurotrophin-binding Trks) to the nucleus is essential for axonal survival. Cortical and hippocampal neurons express the brain-derived neurotrophic factor receptor TrkB (Lindsay et al., 1994). We have shown that hippocampal neurons express both the IC-2C (ubiquitous) and IC-1B (neuron-specific) IC isoforms (Pfister et al., 1996a). When the distribution of TrkB was compared with that of the

Table 1. **GFP-IC-2C dynein motility in PC12 cell neurites**

	Normal	siRNA	NGF
Number of videos	79	21	16
Moving dynein puncta			
Anterograde number (percent of total)	63 (66%)	35 (58%)	14 (48%)
Retrograde number (percent of total)	33 (34%)	24 (42%)	15 (52%)
Total number	96	60	29
Mean anterograde velocity ( $\mu\text{m/s}$ ) [ <i>n</i> ]	$0.9 \pm 0.02$ [849]	$0.7 \pm 0.02$ [444]	$0.9 \pm 0.03$ [173]
Mean retrograde velocity ( $\mu\text{m/s}$ ) [ <i>n</i> ]	$0.9 \pm 0.03$ [300]	$0.8 \pm 0.03$ [329]	$1.2 \pm 0.05$ [140]
Observation time (s)	1,600	320	420
Frequency (motile puncta per second)	0.049	0.050	0.050

GFP-IC-2C dynein puncta moving in PC12 cell neurites were classified according to their direction of movement; the number of puncta in each category and their relative percentages are indicated. Interval velocities were calculated for every movement between each pair of video frames and averaged. The mean velocity ( $\mu\text{m/s}$ ) and number of movements for each category are indicated. Normal, PC12 cells grown under standard conditions; NGF, data collected from PC12 cells within 10 min of addition of NGF to starved cells; siRNA, PC12 cells transfected with the gene 2 siRNA oligonucleotide.

two different dynein complexes in living hippocampal neurons, a significant difference in the extent of colocalization was observed ( $P < 0.005$ ; Fig. 7 A). Only  $2.6 \pm 1.5\%$  of the IC-2C spots colocalized with TrkB, whereas  $17.8 \pm 4.6\%$  of the IC-1B colocalized with TrkB. Thus, dynein containing IC-1B was much more likely to colocalize with TrkB carrier vesicles than dynein containing IC-2C. Significantly, coordinate movement of TrkB with dynein containing IC-1B was also observed, demonstrating that dynein with the IC-1B isoform is responsible for the retrograde transport of TrkB containing endosomes (Fig. 7 B and Video 5, available at <http://www.jcb.org/cgi/content/full/jcb.200803150/DC1>). In contrast, transport of TrkB containing endosomes by dynein containing IC-2C was not found in axons. To confirm that TrkB did not associate with IC-2C dynein complexes, signaling endosomes were immunopurified from the cortex, a brain region with high levels of TrkB expression, by using magnetic beads coupled with anti-Trk antibodies. Antibodies that distinguish between IC isoforms were used to demonstrate that dynein complexes containing IC-1 copurified with the Trk containing vesicles, but dynein containing IC-2 did not (Fig. 7 C). Thus, TrkB ves-

icles from cortical neurons were associated with IC-1 but were not associated with any IC-2 isoform. Together, the live cell imaging and biochemical data demonstrate that dynein complexes containing IC-1B but not dynein containing IC-2C are responsible for the transport of TrkB containing signaling endosomes in cortical and hippocampal neurons.

PC12 cells express the NGF receptor TrkA. Because PC12 cells do not express IC-1 isoforms, we tested the hypothesis that IC-2C-containing dynein was involved in the transport of TrkA signaling endosomes in these cells. We compared the distribution of GFP-IC-2C-containing dynein complexes and TrkA in PC12 cell neurites. After IC-2-specific siRNA was used to deplete the endogenous IC-2 pool, we found significant overlap in the distributions of dynein and TrkA in PC12 cell neurites (Fig. 8 A). NGF binding to the extracellular domain of TrkA leads to autophosphorylation of its cytoplasmic tail, and the activated Trk is internalized with bound NGF in signaling endosomes. Dynein also colocalized with activated (phosphorylated) TrkA in neurites (Fig. 8 B). To confirm the binding of GFP-IC-2C-containing dynein to TrkA, signaling endosomes were immunopurified using antibodies to

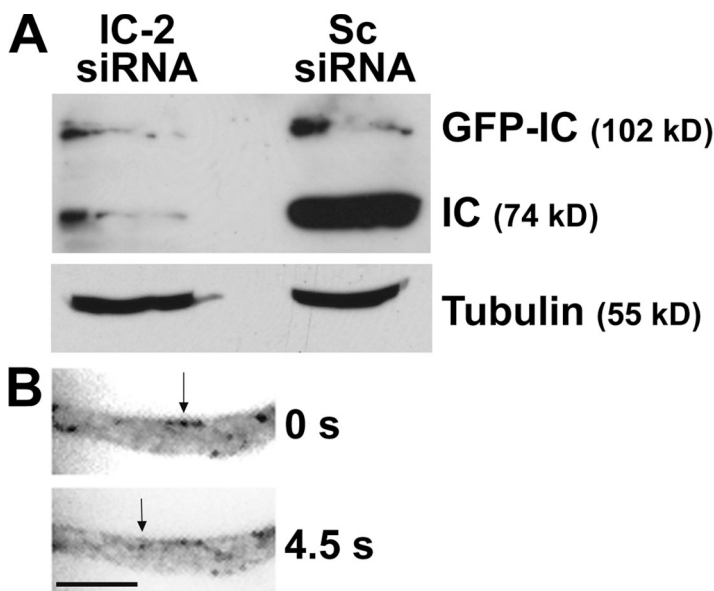


**Figure 4. Retrograde movement of dynein complexes containing IC-2C in siRNA-treated PC12 cell neurites.** (A) Knockdown of endogenous ICs but not GFP-IC by siRNA. The GFP-IC-2C stable PC12 cell line was transfected with either siRNA oligonucleotides to the 3' untranslated region of the rat IC-2 gene (IC-2 siRNA) or control siRNA (Sc siRNA) by electroporation. The cells were grown for 72 h after transfection, and cell lysates were analyzed by SDS-PAGE and Western blotting. The blot was probed with the pan IC antibody (74.1) to identify the endogenous ICs (IC) and the GFP-IC-2C (GFP-IC), and, for a loading control, a tubulin antibody (Tubulin). (B) Retrograde dynein movement in siRNA-treated PC12 cell neurites. IC-2 siRNA-transfected PC12 cells with stable expression of GFP-IC-2C were grown on coverslips and differentiated by the addition of NGF. 72 h after transfection, the dynein motility was imaged. The panels show a video of a portion of a PC12 cell neurite (Video 2, available at <http://www.jcb.org/cgi/content/full/jcb.200803150/DC1>). The arrows indicate one puncta with retrograde movement between the two frames. The time between the video panels is indicated on the right. Although not identified with arrows, many other puncta were moving in the anterograde and retrograde directions. Bar, 5  $\mu\text{m}$ .

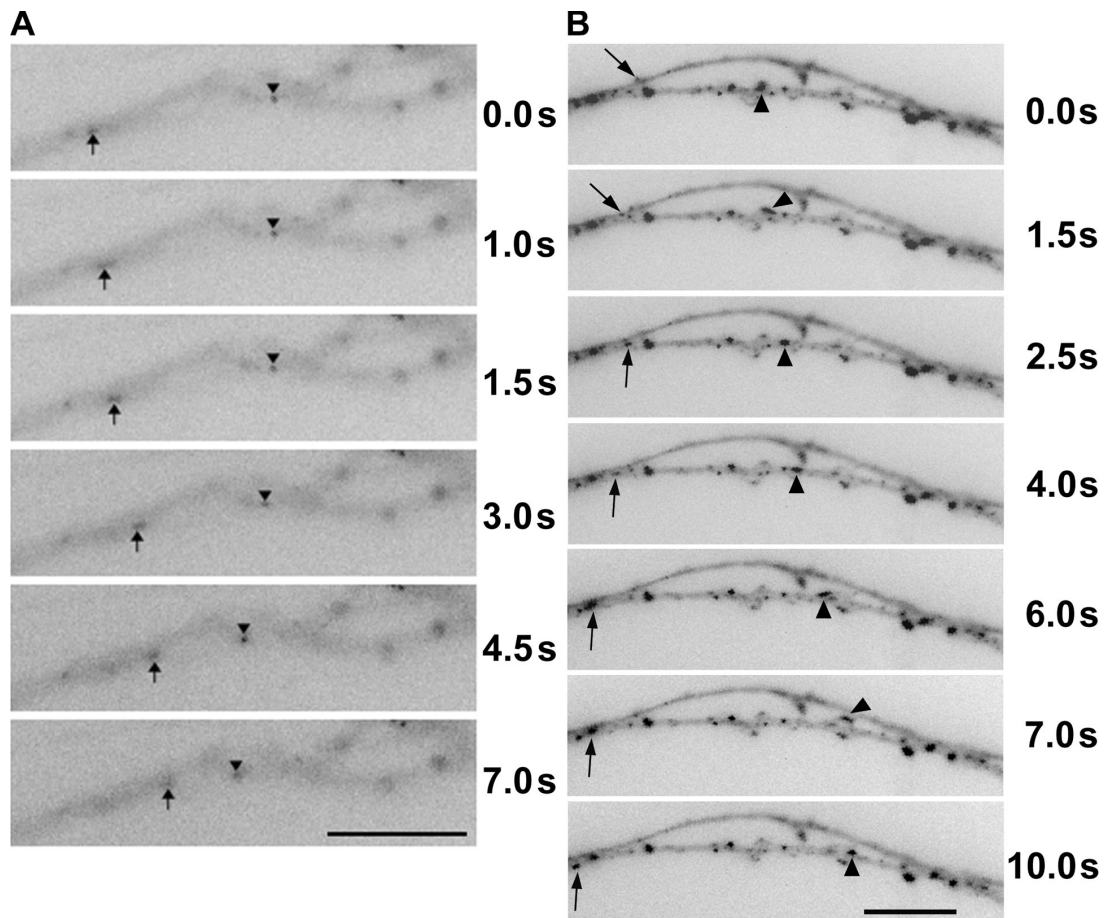


Figure 5. **Bidirectional movement of dynein complexes containing IC-2C and IC-1B in neurons.** (A) IC-2C dynein. Individual frames of a video (Video 3, available at <http://www.jcb.org/cgi/content/full/jcb.200803150/DC1>) showing the movement of dynein puncta in an axon of a cultured hippocampal neuron transfected with mRFP-IC-2C. (B) IC-1B dynein. Individual frames of a video (Video 4) showing movement of dynein puncta in an axon of a cultured hippocampal neuron transfected with mRFP-IC-1B. Arrowheads indicate a puncta moving in the anterograde direction and arrows indicate a puncta moving in the retrograde direction. The time of each frame from the first is indicated on the right. Bars, 10  $\mu$ m.

GFP bound to magnetic beads. TrkA was found to coimmunoprecipitate with the GFP-IC-2C dynein (Fig. 8 C).

We next sought to determine if the addition of NGF to PC12 cells modulated the interaction of dynein with TrkA. Membrane-bounded organelles from control and NGF-stimulated PC12 cells were isolated by immunoaffinity purification with antibodies to dynein on magnetic beads. More activated TrkA copurified with dynein from NGF-stimulated cells than from control cells (Fig. 9 A). This demonstrated that the newly formed signaling endosomes recruited dynein for retrograde transport. We previously found that the addition of NGF increased the phosphorylation of PC12 cell ICs (Salata et al., 2001). We therefore investigated whether the addition of NGF regulated the kinetic properties of dynein containing GFP-IC-2C in the stable PC12 cell line. The addition of NGF significantly increased the mean interval velocity of the dynein puncta moving in the retrograde direction by  $\sim 30\%$ , from 0.9 to 1.2  $\mu$ m/s ( $P < 0.00017$ ), but there was no change in the anterograde interval velocity (Fig. 9 B and Table I). Also, there was a significant increase in the relative amount of dynein puncta moving in the retrograde direction, an increase from 34 to 52% ( $P < 0.0002$ ) upon the addition of NGF (Fig. 9 B and Table I).

These data indicate that NGF stimulation of PC12 cells leads to increased association of activated TrkA containing organelles with dynein and increased dynein retrograde motor activity.

## Discussion

Cytoplasmic dynein is the motor for microtubule minus end-directed (retrograde) transport. Because all cytoplasmic dynein complexes contain the same motor domain, it has been hypothesized that the isoforms of the other subunits were involved in linking specific cargoes to the dynein complex and/or for specific regulation of the dynein motor activity. Supporting this hypothesis, we have shown that dynein complexes that contain the neuron-specific IC IC-1B bind to and transport TrkB containing endosomes. In contrast, dynein complexes containing the ubiquitous IC IC-2C did not associate with or transport the TrkB signaling endosomes. Thus, although neurons express several IC isoforms, only dynein complexes with a specific IC (IC-1B) were used in the transport of TrkB. Interestingly, almost 20% of the IC-1B-containing dynein was used for signaling endosome transport. This is a relatively large amount to be used for the retrograde transport of

Table II. Comparison of the motility of IC-1B and IC-2C dynein in cultured hippocampal neurons

	1B dynein	2C dynein
Number of videos	42	33
Puncta number (percentage of total)		
Total	857	757
Stationary <sup>a</sup>	431 (50%)	481 (63%)
Jiggling movement	274 (32%)	178 (24%)
Excursive movement	152 (18%)	98 (13%)
Direction of excursive movement		
Number (relative percentage)		
Anterograde	69 (45%)	44 (45%)
Retrograde	58 (38%)	40 (41%)
Bidirectional	25 (16%)	14 (14%)
Observation time (s)	840	660
Frequency (motile puncta per second)	0.507	0.418

Hippocampal neurons were transfected with either mRFP-IC-2C or mRFP-IC-1B, and dynein movement was imaged in axons 48 h later. Each dynein puncta was defined as being one of three classes: stationary, those puncta with no sign of movement; excursive, those puncta with movement greater than one pixel for four frames (1 pixel = 137  $\mu$ m; 1 frame per 0.5 s); or jiggling, puncta whose side-to-side oscillatory motion did not meet the criteria for an excursion. Puncta that showed excursive movement were then defined as those moving exclusively anterograde, exclusively retrograde, or those that show bidirectional movement. The number of puncta in each category and the relative frequency are indicated.

<sup>a</sup>More IC-2C dynein puncta are stationary than IC-1B dynein puncta;  $P < 0.0005$ ,  $\chi^2$  test).

a single class of organelle, especially considering that the pool includes dynein being transported in the anterograde direction. In contrast, in PC12 cells, the highly related receptor tyrosine kinase, TrkA, bound to and was transported by dynein complexes containing the IC-2C IC. Together these data indicate that neuronal-specific dynein isoforms are used in neurons for transporting particular critical cargoes.

The mechanism by which the ICs specify the distinct dynein complexes that associate with the different Trk signaling endosomes remains to be determined. It has been suggested that one of the cytoplasmic dynein light chains, DYNLT1 (previously called Tctex1), binds to all three Trk growth factor receptors (Yano et al., 2001). However, we have found that the DYNLT1 light chain binds to all six ICs (Lo et al., 2007b). Thus, DYNLT1 does not provide the specificity necessary to account for our findings. The observation that kinase-dead TrkB-GFP is not transported toward the cell body (Heerssen et al., 2004) suggests that Trk kinase activity is important for dynein transport. One function of the alternative splicing of the ICs may be to generate unique phosphorylation sites to regulate dynein activity (Vaughan and Vallee, 1995). It is tempting to speculate that IC phosphorylation by a downstream effector of the Trk kinases also leads to the recruitment of the appropriate dynein isoform. This hypothesis is consistent with our observation that NGF, which binds to the TrkA receptor, stimulates increased IC phosphorylation (Salata et al., 2001) and, as shown here, increased retrograde dynein activity in PC12 cells.

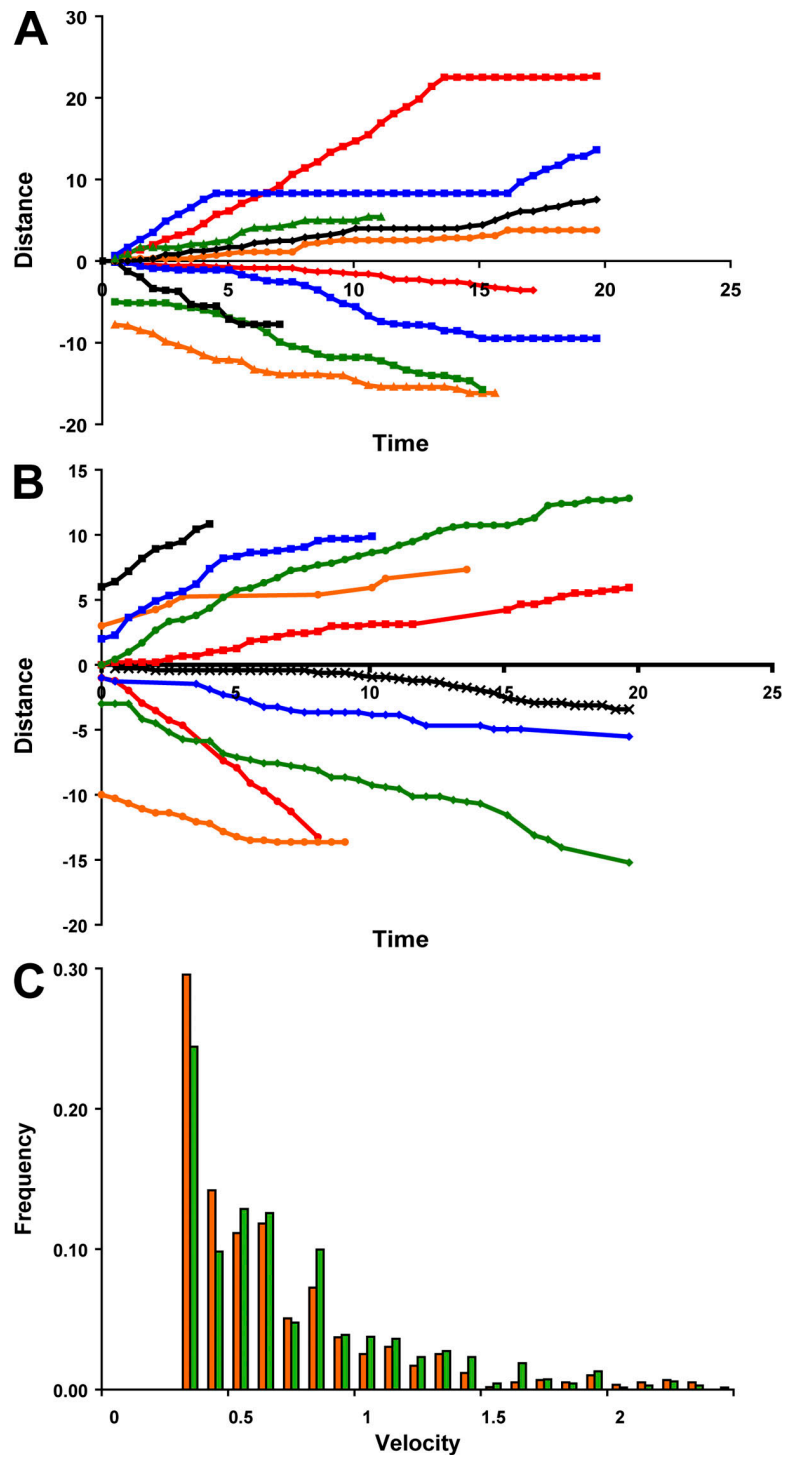
Dynein complexes with GFP-ICs displayed ATP-sensitive microtubule binding and copurified with membrane-bounded organelles. We further found that the copurification of dynein

complexes and Trks required the presence of a membranous organelle (unpublished data). In addition, we demonstrated specific differences in the motor activities of dynein complexes containing the distinct IC isoforms. When the kinetics of retrograde dynein motor complexes containing IC-2C and IC-1B were compared, we found that IC-2C-containing dynein complexes were less likely to be motile. Although the two complexes had identical interval velocity distributions, the excursions of IC-1B-containing dynein complexes were, on average, of longer duration. These data suggest that the different ICs isoforms do modulate dynein motor activity. They are also consistent with the recent finding that the phenotype of dynein motor mutations in the *Caenorhabditis elegans* were suppressed by the deletion of specific cargo-binding subunit isoforms (O'Rourke et al., 2007). Together, the data support the hypothesis that the subunit isoforms differentially regulate dynein activity. In contrast to our observations of IC-2C in PC12 cells, there was no significant difference in the number of IC-2C and IC-1B dynein puncta moving in the anterograde and retrograde directions in axons. The neuronal dynein puncta were observed to switch directions but there was no preference for a specific change in direction for either dynein variant.

When we compared the anterograde kinetics of dynein complexes with the two distinct IC isoforms in cultured embryonic hippocampal axons, no difference was observed in the interval velocity distribution of the two dynein complexes. However, a small but statistically significant difference ( $P < 0.02$ ; Table III) was observed in the mean anterograde excursion velocities; dynein with IC-1B moved slower in cultured hippocampal neurons. We previously found that in adult rat optic nerves, dynein with IC-2C was transported in the anterograde fast transport, whereas dynein complexes with IC-1B were transported in the anterograde slow component b (Dillman et al., 1996). Transport of IC-2C dynein complexes in the anterograde fast component suggested that they were transported as cargo by a member of the kinesin family. Consistent with this, an overlap in the distributions of GFP-IC-2C and Kinesin-1 was observed when monomeric red fluorescent protein (mRFP)-Kinesin-1 (Kif5a) was transfected into PC12 cells, and Kinesin-1 was present when organelles were purified from the GFP-IC-2C cell line by immunoaffinity purification with antibodies to GFP (unpublished data). Although the anterograde kinetics of IC-1B dynein observed in cultured embryonic hippocampal neurons were more rapid than those observed in the axons of adult optic nerve, it is notable that our results are consistent with recent observations of the transport of slow component b proteins in hippocampal neurons (Roy et al., 2007). A-synuclein and two other slow component b proteins were transported at velocities comparable those of dynein containing IC-1B.

Other isoforms of dynein subunits have been implicated in linking dynein to specific cargo; e.g., light IC 1 (DYNCL1I1) binds to pericentrin and DYNLT1 binds to rhodopsin, whereas DYNLT3 binds to Bub3 (Tai et al., 1999; Tynan et al., 2000; Reilein et al., 2003; Vallee et al., 2004; Lo et al., 2007a). The IC subunit is involved in binding dynein to cargoes through its interaction with the p150 subunit of dynactin (Karki and Holzbaur,

**Figure 6. Comparison of the motility of dynein complexes containing IC-2C and IC-1B in neurons.** (A) Displacement tracking of IC-2C dynein. The positions of representative individual dynein puncta were tracked along the neurite in each frame of the videos, and the linear displacements (in micrometers) of 10 individual dynein puncta were graphed against time (in seconds). Anterograde movement is recorded as positive and retrograde movement as negative displacement. (B) Displacement tracking of IC-1B dynein. The positions of representative individual dynein puncta were tracked along the axon in each frame of the videos, and the linear displacements of 10 individual dynein puncta are graphed against time of movement. Anterograde movement is recorded as positive and retrograde movement as negative displacement. The initial positions of many of the puncta were set at 0, whereas the initial displacements of the some puncta were offset on the y axis to distinguish them on the graph. (C) Comparison of the retrograde interval velocity distributions of dynein complexes with the IC-2C and IC-1B isoforms in neurons. Velocities ( $\mu\text{m/s}$ ) of individual retrograde movements of GFP-IC-2C dynein puncta between two frames were plotted against the frequency of their occurrence. Orange, IC-2C dynein ( $n = 592$ ); green, IC-1B dynein puncta ( $n = 692$ ).



1995; Vaughan and Vallee, 1995). The IC also binds some cargoes directly (Ligon et al., 2004; Caviston et al., 2007). The results presented here demonstrate for the first time that specific dynein variants defined by different ICs isoforms are responsible for the transport of specific membrane-bounded organelles. Interestingly, although the chromaffin-derived PC12 cells make use of the ubiquitous IC isoform IC-2C for Trk signaling endosome transport, neurons that express IC-2C use a different IC isoform for Trk transport, one which is expressed exclusively in neurons. Therefore it will be important to identify and compare

the regulatory pathways in the different cell types to understand the mechanisms involved in the recruitment of the different dynein complexes to signaling endosomes.

## Materials and methods

**Establishment of the PC12 cell line with the stable expression of GFP-IC-2C**  
Rat pheochromocytoma—PC12 cells—cultured in DME (Invitrogen) with 5% FBS and either 10% equine serum or FCS (all from Thermo Fisher Scientific) and gentimycin were transfected with the GFP-IC-2C plasmid using Fugene 6 (Roche), and cells with stable expression of the plasmids were



Table III. Kinetic parameters of IC-1B and IC-2C dynein movement in hippocampal neurons

	1B dynein	2C dynein
Number of dynein puncta	152	98
Retrograde		
Mean interval velocity $\mu\text{m/s}$ [ <i>n</i> ]	0.7 $\pm$ 0.02 [692]	0.7 $\pm$ 0.02 [592]
Excursions		
Number	94	49
Mean velocity ( $\mu\text{m/s}$ )	0.6 $\pm$ 0.04	0.7 $\pm$ 0.05
Mean distance ( $\mu\text{m}$ )	2.7 $\pm$ 0.24	2.3 $\pm$ 0.25
Mean time (s) <sup>a</sup>	4.8 $\pm$ 0.33	3.4 $\pm$ 0.2
Pauses		
Number	42	55
Average time (s) <sup>b</sup>	4.6 $\pm$ 0.49	3.3 $\pm$ 0.24
Anterograde		
Average interval velocity $\mu\text{m/s}$ [ <i>n</i> ]	0.7 $\pm$ 0.02 [1,061]	0.7 $\pm$ 0.02 [590]
Excursions		
Number	128	47
Mean velocity ( $\mu\text{m/s}$ ) <sup>c</sup>	0.6 $\pm$ 0.03	0.7 $\pm$ 0.05
Mean distance ( $\mu\text{m}$ )	2.6 $\pm$ 0.18	3.0 $\pm$ 0.51
Average time (s)	4.8 $\pm$ 0.29	3.7 $\pm$ 0.34
Pauses		
Number	56	59
Mean time (s)	4.0 $\pm$ 0.27	4.5 $\pm$ 0.43

Interval velocities for dynein complexes with mRFP-IC-2C or mRFP-IC-1B moving in hippocampal neuronal axons were calculated for every movement between each pair of video frames and averaged. Excursions are puncta movements greater than one pixel for four frames (1 pixel = 137  $\mu\text{m}$ ; 1 frame per 0.5 s). Excursion velocity is total distance traveled per total time traveled. Pauses are periods with no dynein movement that separate two excursions.

<sup>a</sup>Retrograde IC-1B dynein has excursions with longer mean durations than dynein with IC-2C ( $P < 0.0003$ , Student's *t* test).

<sup>b</sup>Retrograde IC-1B dynein pauses for longer mean times than dynein with IC-2C ( $P < 0.01$ , Student's *t* test).

<sup>c</sup>The mean velocity of anterograde IC-2C dynein is faster than that of dynein with IC-1B ( $P < 0.02$ , Student's *t* test).

selected with G418 (Invitrogen). Colonies of cells surviving drug selection were cloned by limiting dilution and screened for low-level expression of GFP-IC-2C by fluorescence microscopy.

#### Biochemical characterization of dynein with GFP-ICs

Microtubule binding: GFP-IC-expressing cells were homogenized in cold PHEM (50 mM Pipes, 50 mM Hepes, 2mM  $\text{MgCl}_2$ , 1mM EGTA, and protease inhibitors) and centrifuged at 32,000 *g* for 5 min in a centrifuge (120.2 rotor; Optima TLX; Beckman Coulter), and the resulting soluble fraction, supernatant S1, was retained. Then, purified tubulin prepared as described previously (Dillman et al., 1996) was polymerized with 10  $\mu\text{M}$  taxol (EMD), and microtubules were added to the S1 to a final concentration of 0.25 mg/ml and incubated at 37°C for 15 min. The microtubules were centrifuged through a 10% sucrose cushion in PHEM at 22,000 *g* for 20 min at 27°C. The microtubule pellet was resuspended in 10 mM Mg-ATP in PHEM for 10 min and centrifuged at 36,000 *g* for 20 min, resulting in a supernatant and pellet. Sucrose gradient centrifugation of the S1 (unpurified dynein) was performed as described previously (Lo et al., 2007b). Blots were probed with the dynein IC and GFP antibodies as described previously (Lo et al., 2006). The intensities of the IC and GFP-IC bands in Fig. 2 were quantified by densitometry with ImageQuant (MDS Analytical Technologies).

#### Isolation of membrane bound organelles

Membrane-bound organelles were isolated from control and activated PC12 cells using the method described previously (Grimes et al., 1996). In brief, cells were homogenized in a cytoplasm-like buffer (38 mM each of the potassium salts of aspartic, gluconic, and glutamic acids; 20 mM MOPS; 5 mM reduced glutathione; 10 mM potassium bicarbonate; 0.5 mM magnesium carbonate; 1 mM EGTA; 1 mM EDTA, pH 7.1; 1 mM sodium orthovanadate; and protease inhibitors [1 mM PMSF, 10  $\mu\text{g/ml}$  benzamidine, 1  $\mu\text{g/ml}$  pepstatin, 1  $\mu\text{g/ml}$  leupeptin, and 1  $\mu\text{g/ml}$  aprotinin]), the nuclear and cell pellet (P1) was discarded, the supernatant (S1) was further fractionated by centrifugation at 100,000 *g* for 1 h, and the membrane fraction (P2) was resuspended and incubated with protein A magnetic beads (DynaBeads, Invitrogen) preloaded with either an antibody or the control IgG as indicated in the figures. After the binding step, the beads were washed and analyzed

by SDS-PAGE and Western blotting and probed with the indicated antibodies. Membrane-bound organelles were isolated from rat brain cortex using the method described previously (Steggmaier et al., 1999), and brain cortices were homogenized with a Teflon homogenizer in homogenization buffer (20 mM Hepes, pH 7.4, 10 mM sucrose, 120 mM KCl, 2 mM EDTA, 2 mM EGTA, 6 mM MgCl, and 1 mM DTT).

#### Cell culture and transfection

Embryonic hippocampal neurons were grown on 18-mm-diameter coverslips (Thermo Fisher Scientific) and either inverted over glia in media (Goslin et al., 1998) and transfected on day 6 or 7 in vitro with calcium phosphate (Zhang et al., 2003) or maintained in serum-free media with B-27 supplement (Invitrogen; Winckler et al., 1999) and transfected at day 10 in vitro with Lipofectamine 2000 (Invitrogen). PC12 cells were grown on the same coverslips and differentiated for 4 d by the addition of 50 U/ml of NGF (Millipore), and sodium butyrate was added 16 h before imaging (Sambrook and Russell, 2001). For some experiments, the differentiated PC12 cells were starved for 2 h, NGF was added, and the dynein motility was imaged within 10 min after the readdition of NGF. Immunocytochemistry was performed as described previously (Lo et al., 2007a) except that the cells were permeabilized after fixation. Cy3- and FITC-labeled secondary antibodies (Jackson ImmunoResearch Laboratories) were used to detect the indicated primary antibodies, and coverslips were mounted with the Prolong Antifade kit (Invitrogen).

#### Live cell imaging

Coverslips with differentiated PC12 cells or primary hippocampal neurons were placed in a custom-made chamber with culture medium and imaged on a temperature-controlled stage (35°C) with a microscope (Diaphot TMD; Nikon) equipped with external exciter and emission filter wheels and internal dichroic filters (matched sets for GFP and mRFP or Cy3; Chroma Technology Corp.). Videos were collected with a 100 $\times$  lens (NA 1.4; Nikon) using a CoolSnap ES camera and, as appropriate, a DualView camera (both from Roper Scientific) for 20 s; exposure times were 0.5 s in streaming mode with 2  $\times$  2 binning, (except that Video 1 has 1  $\times$  1 binning and a length of 40 s). The shutters, filter wheels, and camera were coordinated by MetaMorph6 (MDS Analytical Technologies). Videos were

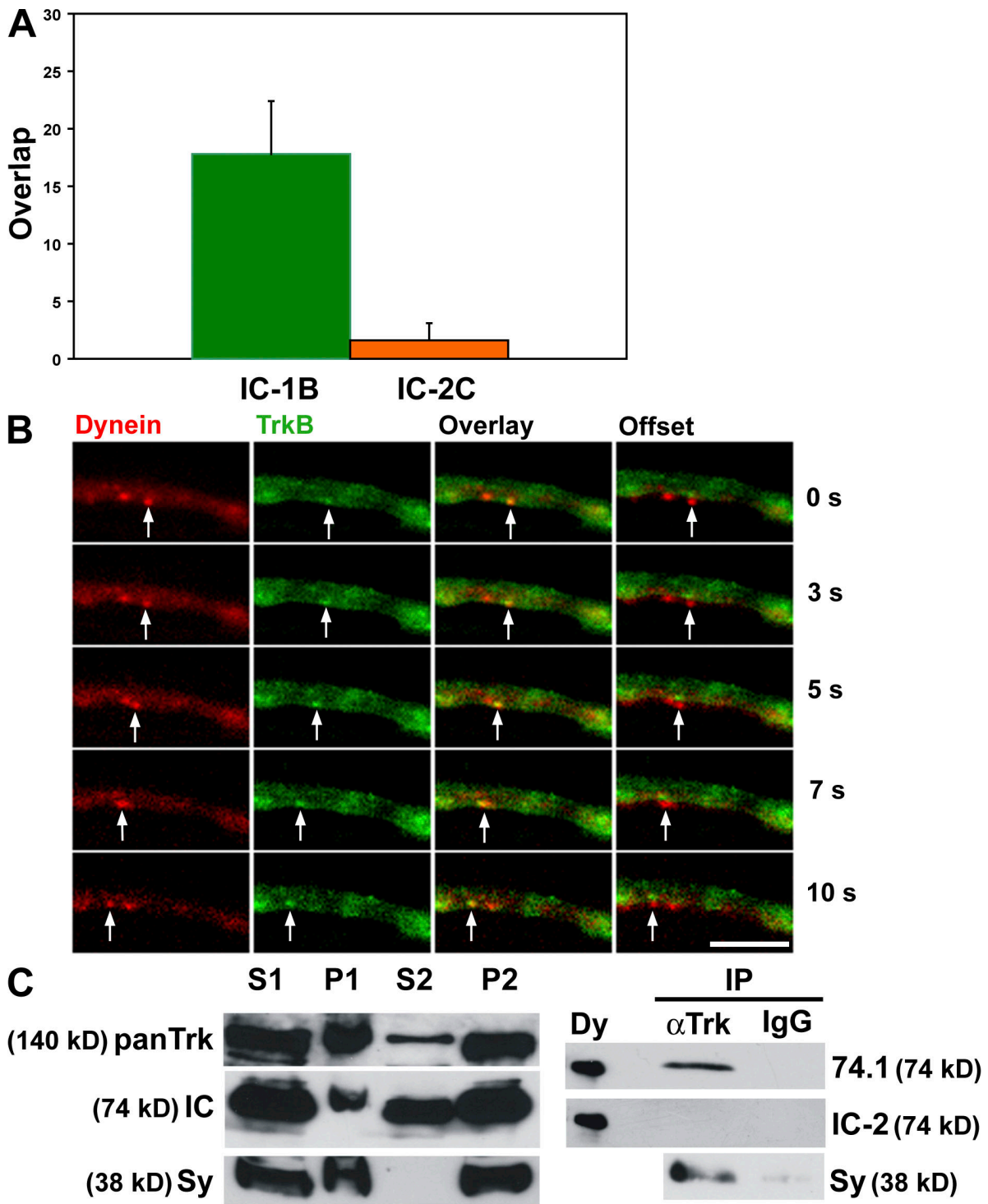


**Figure 7. Coordinate movement of TrkB and cytoplasmic dynein complexes containing IC-1B in neurons.** (A) Comparison of the colocalization of TrkB with IC-2C and IC-1B dynein complexes. Hippocampal neurons were cotransfected with TrkB-GFP and either mRFP-IC-2C or mRFP-IC-1B and imaged in living cells; the number of dynein, Trk, and overlapping puncta was then determined in the transfected neurons. The percentages of dynein puncta that colocalized with TrkB were determined for each neuron, averaged, and graphed with the standard error. Dynein containing IC-1B (green) was significantly more likely ( $P < 0.005$ , Student's *t* test) to be associated with the TrkB carrier vesicles than dynein containing IC-2C (orange). 15 IC-1B-transfected neurons were analyzed; a total of 211 dynein puncta and 270 TrkB puncta were counted, and 41 of the puncta were colocalized. 10 IC-2C-transfected neurons were analyzed; a total of 302 dynein puncta and 282 TrkB puncta were counted, and 10 of the puncta were colocalized. (B) Live cell imaging. Hippocampal neurons were cotransfected with TrkB-GFP and mRFP-IC-1B. TrkB-GFP (green) and mRFP-dynein image sets were collected simultaneously as described in the Materials and methods. The panels are individual frames derived from Video 5 (available at <http://www.jcb.org/cgi/content/full/jcb.200803150/DC1>). The coordinately moving spots are indicated with white arrows. Panels from left to right: (Dynein) movement of the dynein puncta (red); (TrkB) movement of TrkB puncta (green); (Overlay) overlay of the dynein (red) and TrkB (green) puncta, the moving yellow puncta is indicated with an arrow; (Offset) vertical offset of the dynein puncta (red, bottom) and TrkB puncta (green, top) to more clearly demonstrate the coordinate movement of the two proteins. The time interval for each frame from the start of the video is indicated on the right. Bar, 10  $\mu$ m. (C) IC-1 dynein is preferentially associated with Trk containing

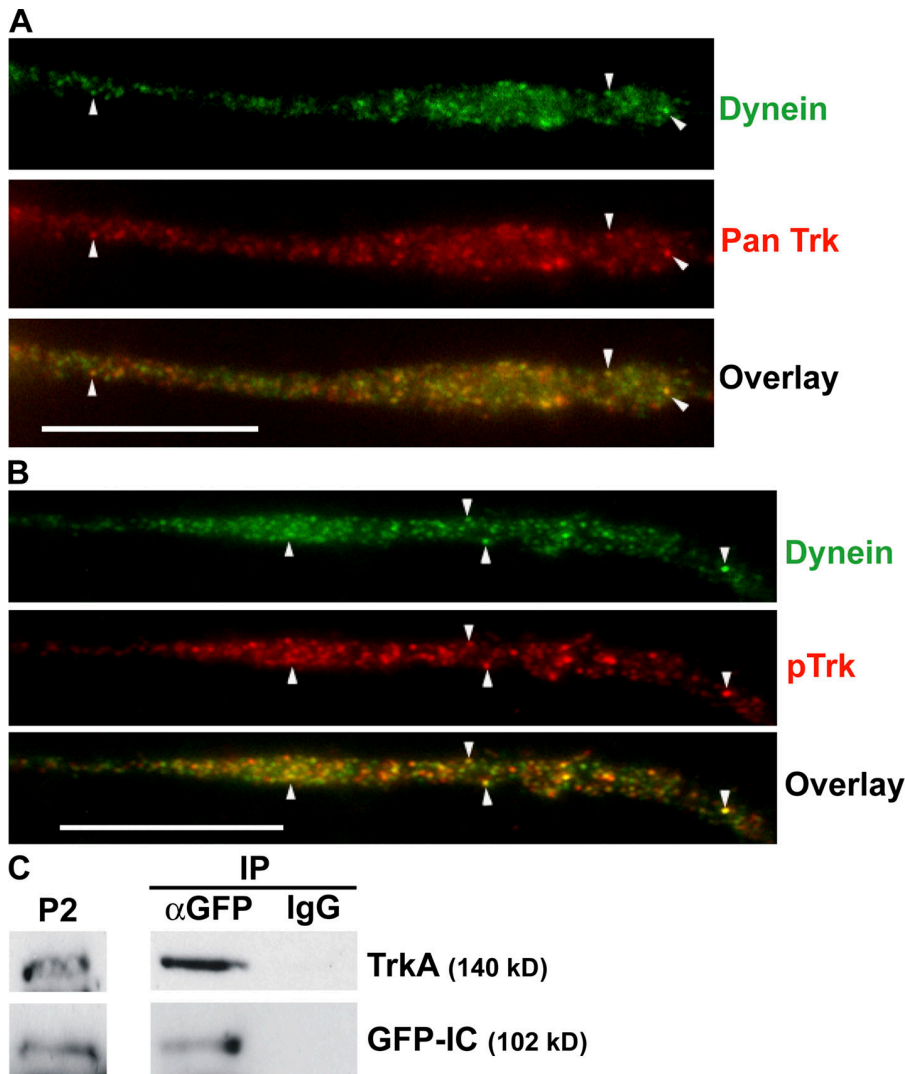


**Figure 8. TrkA signaling endosomes associate with IC-2C dynein complexes in PC12 cells.** (A) Colocalization of dynein and the TrkA growth factor receptor in PC12 cells. Neurite of a stable GFP-IC-2C PC12 cell treated with siRNA stained with dynein pan IC antibody, 74.1 (Dynein, green) and a pan Trk antibody (Pan Trk, red), and the overlay of the two colors. Arrowheads indicate some of the colocalizing puncta. (B) Colocalization of dynein and activated TrkA growth factor receptor in PC12 cells. Neurite of stable GFP-IC-2C cell line treated with siRNA stained with dynein pan IC antibody, 74.1 (dynein, green), and an antibody that reacts with activated (phosphorylated) Trk (pTrk, red). Arrowheads indicate some of the colocalizing puncta. Bar, 10  $\mu$ m. (C) GFP-IC-2C-containing dynein is associated with TrkA containing organelles in PC12 cells. The membrane fraction (P2) was prepared from NGF-stimulated PC12 cells as described for Fig. 2, and GFP-IC-containing vesicles were isolated by immunoaffinity purification on magnetic beads laded with antibodies to GFP. The anti-GFP ( $\alpha$ -GFP) and control IgG beads were washed, and the bound proteins were analyzed by SDS-Page and Western blotting with pan Trk antibody and the pan IC antibody, 74.1. The presence of GFP-IC (GFP-IC) on the beads was a positive control.

cropped and autoscaled with MetaMorph6. QuickTime (Apple) videos were labeled and compressed with Keynote (Apple) and are displayed at 10 frames per second. Individual video frames were cropped and scaled in MetaMorph; image Tif files were arranged for presentation with Photoshop 7 (Adobe) using the auto levels, levels, brightness/contrast, or curves functions and labeled with Illustrator CS (Adobe).

#### Motility analyses

Discrete interval movement velocities between each pair of video frames were calculated and graphed as described previously (Kieran et al., 2005) except that the puncta were tracked manually. Excursions are defined as puncta movements greater than one pixel for four frames. The standard pixel size was 0.138  $\mu$ m, the exposure time was 0.5 s, and the smallest detectable velocity was 0.3  $\mu$ m/s. Motile fluorescent dynein puncta were spots with two or three bright pixels. In the GFP-IC-2C PC12 cell line, the puncta intensities were  $\sim$ 20% above background; in the siRNA-treated PC12 cell line and in the transiently transfected neurons, the puncta intensities were 60–90% above background. The difference in background may account for the observation that the mean interval velocity of dynein

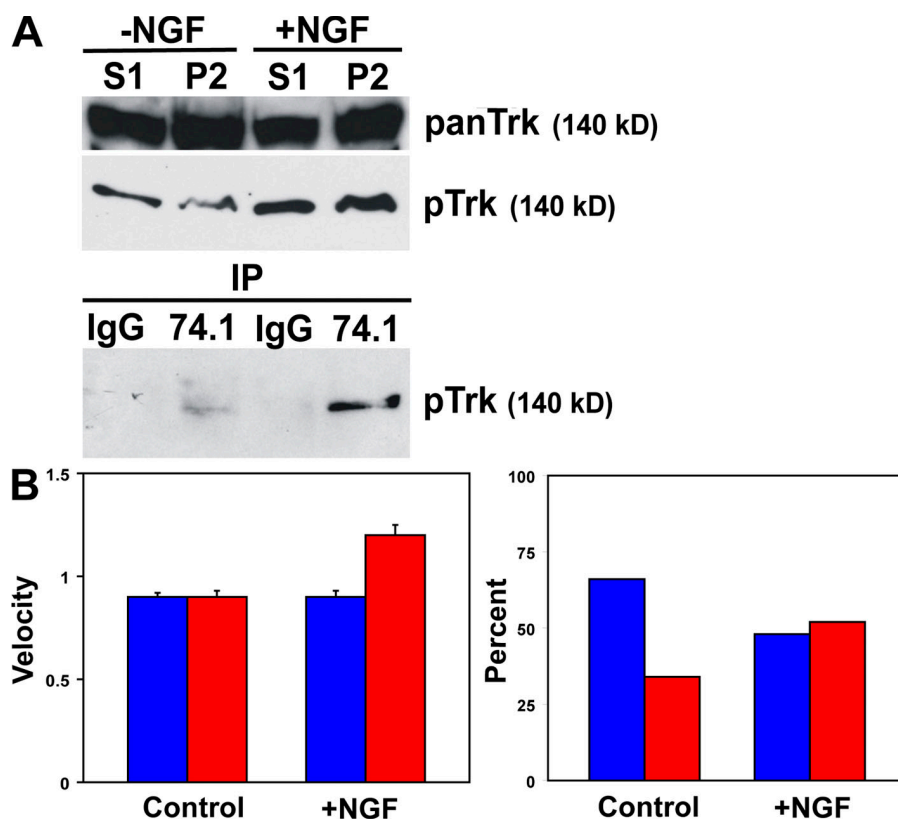
in normal PC12 cell neurites was larger than that observed in the siRNA-treated PC12 cell neurites and or hippocampal axons. The higher background levels may obscure the slower movements. In addition, axons have a smaller diameter than the PC12 cell neurites. This minimizes loss of puncta due to their moving out of the plane of focus. The smaller diameter also may lead to more collisions with other puncta or other unlabeled obstructions. We occasionally observed collisions between puncta in axons and puncta leaving a group of stationary puncta. The formation of EB3 “comets” upon binding to growing microtubule plus ends was used to determine the polarity orientation of microtubules in PC12 cell neurites using the method described previously (Stepanova et al., 2003)

#### Antibodies, plasmids, and siRNA

The following antibodies were used: monoclonal pan anti-IC, 74.1 (Dillman and Pfister, 1994); polyclonal anti-IC 2 isoform, IC-2 (Vaughan and Vallee, 1995; Pfister et al., 1996a,b); anti-phospho-Trk, DF49 (Segal et al., 1996) and E-6 (pT490; Santa Cruz Biotechnology; Jullien et al., 2003); anti-panTrk, DF18 (Segal et al., 1996) and B3 (Santa Cruz Biotechnology, Inc.; Bronfman et al., 2003; Arevalo et al., 2006); monoclonal anti-tubulin,

vesicles from brain cortex. Membrane-bounded organelles were isolated from fresh rat brain cortex, and the fractions were analyzed by SDS-PAGE and Western blotting; the postnuclear supernatant (S1) and pellet (P1), high-speed supernatant (S2), and high-speed membrane fraction (P2) are indicated. The presence of Trks, ICs, and synaptophysin (Sy) in the fractions was determined by probing the blots with antibodies to Trk and synaptophysin and the pan IC antibody, 74.1. Trk containing organelles were purified by immunoaffinity purification on magnetic beads from the membrane fraction (P2) with antibodies to Trk ( $\alpha$ Trk) or control IgG (IgG) and analyzed by SDS-PAGE and Western blotting. The IC isoforms present in the  $\alpha$ -Trk immunoprecipitate were identified by probing the blot with an antibody specific to the IC-2 isoforms (IC-2) followed by the pan IC antibody (74.1). As a positive control for the presence of both IC-1 and IC-2 on the blot, dynein immunoprecipitated from the testis was loaded on a neighboring lane (Dy).

**Figure 9. Regulation of dynein by neurotrophins and Trks.** (A) Recruitment of activated (phosphorylated) TrkA to dynein containing vesicles in NGF-treated PC12 cells. PC12 cells were harvested and then treated with NGF (+NGF) or buffer (-NGF). The postnuclear supernatant (S1) and the membrane fractionant (P2) were prepared and analyzed by SDS-PAGE and Western blotting. The blot was first probed with an antibody specific for the phosphorylated (activated) form of Trk (pTrk). Next, the blot was stripped and probed with pan Trk antibody (panTrk). The vesicle fractions were immunoprecipitated (IP) with anti-pan Trk antibody (74.1) or control IgG (IgG) on magnetic beads, and a Western blot of the proteins bound to the beads was probed with the antibody to activated Trk (pTrk). The blots were probed with a pan Trk antibody as a loading control. (B) Modulation of dynein by NGF. (left) Graphs of mean anterograde (blue) and retrograde (red) interval velocities for control (Control) and NGF-treated (+NGF) PC12 cells. The mean interval retrograde velocity for NGF-stimulated cells was  $1.2 \mu\text{m/s} \pm 0.05$  standard error ( $n = 140$ ), and for control cells  $0.9 \mu\text{m/s} \pm 0.03$  standard error ( $n = 300$ ). The difference in mean retrograde velocities was significant at  $P < 0.00017$  (Student's *t* test). (right) Graph showing the percent of GFP-IC-2C dynein puncta moving in the anterograde (blue) and retrograde (red) directions in control (Control) and NGF-stimulated cells (+NGF). The addition of NGF resulted in a significant increase in the relative number of dynein puncta moving in the retrograde direction ( $P < 0.0002$ ,  $\chi^2$  test).



DM1A (Sigma-Aldrich); monoclonal anti-tubulin, Tu27 (Lee et al., 1990a,b); polyclonal anti-GFP (Invitrogen; Ding et al., 2005); monoclonal anti-GFP (Invitrogen); anti-synaptophysin, SY38 (Millipore; Wiedenmann and Franke, 1985). The GFP-IC-2C plasmid was made by modifying the coding region (a gift of K. Vaughan, University of Notre Dame, Notre Dame, IN) by PCR amplification to include SacI and EcoRI sites and was then cloned into pEGFP-N1 (Clontech Laboratories, Inc.). mRFP-IC-2C was made by replacing the EGFP coding region of EGFP-IC-2C-N1 with the mRFP coding sequence (a gift of R. Tsien, University of California, San Diego, La Jolla, CA; and R. Day, University of Virginia, Charlottesville, VA; Campbell et al., 2002) using the AgeI and BsrGI restriction sites. IC-1B-mRFP (for correct sequence and nomenclature, see Pfister et al., 2005, 2006; Myers et al., 2007) was modified by PCR from rat brain cDNA using the IC-1 cDNA terminal sequences (Paschal et al., 1992) to include SacI and EcoRI restriction sites and cloned into the mRFP vector. TrkB-GFP has been described previously (Watson et al., 1999), and TrkB-mRFP was made by cloning the TrkB coding sequence into the mRFP vector using BamHI and KpnI. Kinesin-1-mRFP (Kif5A) was made by modifying the coding sequence (a gift of G. Morifini and S. Brady, University of Illinois at Chicago, Chicago, IL) to include the restriction sites KpnI and BamHI and was cloned into the mRFP plasmid. mRFP-EB3 was a gift of J. Zhang (University of Medicine and Dentistry of New Jersey, Newark, NJ). The siRNA oligonucleotide to the 3' untranslated region of rat IC-2 (5'-CCCTTTGCTTTGGATTGGTGTCATT-3') and a control siRNA oligonucleotide (5'-GACGGTTATTACAGAAGGACGTA-3') were synthesized by Invitrogen. siRNA transfections were performed in  $2 \times 10^6$  of the GFP-IC-2C PC12 cells using an electroporator (Nucleofector; Amaxa) according to the manufacturer's instructions. Cells were cultured for 72–96 h before subsequent manipulations.

#### Online supplemental material

Video 1 shows bidirectional movement of dynein containing IC-2C in a PC12 cell neurite. Video 2 shows retrograde movement of dynein complexes containing IC-2C in siRNA-treated PC12 cell neurites. Video 3 shows bidirectional movement of dynein complexes containing IC-2C in neurons. Video 4 shows bidirectional movement of dynein containing IC-1B in neurons.

Video 5 shows coordinate movement of TrkB and cytoplasmic dynein complexes containing IC-1B in neurons. Online supplemental material is available at <http://www.jcb.org/cgi/content/full/jcb.200803150/DC1>.

We thank Dr. R.J. Lye for cloning the rat IC-1B cDNA; Dr. S.J. Susalka for construction of the GFP-IC-2C plasmid; Dr. S. Keller for advice with magnetic bead immunopurification; and H. Asmussen, Z. Lasiecka, M. Vakulenko, and Dr. C. Yap for assistance with neuronal culture and transfection.

This work was supported by grants from the National Institutes of Health National Institute of Neurological Disorders and Stroke to K.K. Pfister (NS29996) and R. Segal (NS050674).

Submitted: 27 March 2008

Accepted: 16 May 2008

## References

- Arevalo, J.C., D.B. Pereira, H. Yano, K.K. Teng, and M.V. Chao. 2006. Identification of a switch in neurotrophin signaling by selective tyrosine phosphorylation. *J. Biol. Chem.* 281:1001–1007.
- Bhattacharyya, A., F.L. Watson, S.L. Pomeroy, Y.Z. Zhang, C.D. Stiles, and R.A. Segal. 2002. High-resolution imaging demonstrates dynein-based vesicular transport of activated Trk receptors. *J. Neurobiol.* 51:302–312.
- Bronfman, F.C., M. Tcherpakov, T.M. Jovin, and M. Fainzilber. 2003. Ligand-induced internalization of the p75 neurotrophin receptor: a slow route to the signaling endosome. *J. Neurosci.* 23:3209–3220.
- Campbell, R.E., O. Tour, A.E. Palmer, P.A. Steinbach, G.S. Baird, D.A. Zacharias, and R.Y. Tsien. 2002. A monomeric red fluorescent protein. *Proc. Natl. Acad. Sci. USA.* 99:7877–7882.
- Caviston, J.P., J.L. Ross, S.M. Antony, M. Tokito, and E.L. Holzbaur. 2007. Huntingtin facilitates dynein/dynactin-mediated vesicle transport. *Proc. Natl. Acad. Sci. USA.* 104:10045–10050.
- Delcroix, J.D., J.S. Valletta, C. Wu, S.J. Hunt, A.S. Kowal, and W.C. Mobley. 2003. NGF signaling in sensory neurons: evidence that early endosomes carry NGF retrograde signals. *Neuron.* 39:69–84.

- Dillman, J.F. III, and K.K. Pfister. 1994. Differential phosphorylation in vivo of cytoplasmic dynein associated with anterogradely moving organelles. *J. Cell Biol.* 127:1671–1681.
- Dillman, J.F. III, L.P. Dabney, S. Karki, B.M. Paschal, E.L. Holzbaur, and K.K. Pfister. 1996. Functional analysis of dynactin and cytoplasmic dynein in slow axonal transport. *J. Neurosci.* 16:6742–6752.
- Ding, L., A. Spencer, K. Morita, and M. Han. 2005. The developmental timing regulator AIN-1 interacts with miRISCs and may target the argonaute protein ALG-1 to cytoplasmic P bodies in *C. elegans*. *Mol. Cell.* 19:437–447.
- Goslin, K., H. Asmussen, and G. Banker. 1998. Rat hippocampal neurons in low-density culture. In *Culturing nerve cells*. G. Banker and K. Goslin, editors. The MIT Press, Cambridge, MA. 339–370.
- Grimes, M.L., J. Zhou, E.C. Beattie, E.C. Yuen, D.E. Hall, J.S. Valletta, K.S. Topp, J.H. LaVail, N.W. Bennett, and W.C. Mobley. 1996. Endocytosis of activated TrkA: evidence that nerve growth factor induces formation of signaling endosomes. *J. Neurosci.* 16:7950–7964.
- Habermann, A., T.A. Schroer, G. Griffiths, and J.K. Burkhardt. 2001. Immunolocalization of cytoplasmic dynein and dynactin subunits in cultured macrophages: enrichment on early endocytic organelles. *J. Cell Sci.* 114:229–240.
- Heerssen, H.M., M.F. Pazyra, and R.A. Segal. 2004. Dynein motors transport activated Trks to promote survival of target-dependent neurons. *Nat. Neurosci.* 7:596–604.
- Huang, E.J., and L.F. Reichardt. 2003. Trk receptors: roles in neuronal signal transduction. *Annu. Rev. Biochem.* 72:609–642.
- Jullien, J., V. Guili, E.A. Derrington, J.L. Darlix, L.F. Reichardt, and B.B. Rudkin. 2003. Trafficking of TrkA-green fluorescent protein chimeras during nerve growth factor-induced differentiation. *J. Biol. Chem.* 278:8706–8716.
- Karki, S., and E.L. Holzbaur. 1995. Affinity chromatography demonstrates a direct binding between cytoplasmic dynein and the dynactin complex. *J. Biol. Chem.* 270:28806–28811.
- Kieran, D., M. Hafezparast, S. Bohnert, J.R. Dick, J. Martin, G. Schiavo, E.M. Fisher, and L. Greensmith. 2005. A mutation in dynein rescues axonal transport defects and extends the life span of ALS mice. *J. Cell Biol.* 169:561–567.
- Lee, M.K., L.I. Rebhun, and A. Frankfurter. 1990a. Posttranslational modification of class III beta-tubulin. *Proc. Natl. Acad. Sci. USA.* 87:7195–7199.
- Lee, M.K., J.B. Tuttle, L.I. Rebhun, D.W. Cleveland, and A. Frankfurter. 1990b. The expression and posttranslational modification of a neuron-specific beta-tubulin isotype during chick embryogenesis. *Cell Motil. Cytoskeleton.* 17:118–132.
- Levy, J.R., and E.L. Holzbaur. 2006. Cytoplasmic dynein/dynactin function and dysfunction in motor neurons. *Int. J. Dev. Neurosci.* 24:103–111.
- Ligon, L.A., M. Tokito, J.M. Finklestein, F.E. Grossman, and E.L. Holzbaur. 2004. A direct interaction between cytoplasmic dynein and kinesin I may coordinate motor activity. *J. Biol. Chem.* 279:19201–19208.
- Lindsay, R.M., S.J. Wiegand, C.A. Altar, and P.S. DiStefano. 1994. Neurotrophic factors: from molecule to man. *Trends Neurosci.* 17:182–190.
- Lo, K.W., H.M. Kan, and K.K. Pfister. 2006. Identification of a novel region of the cytoplasmic Dynein intermediate chain important for dimerization in the absence of the light chains. *J. Biol. Chem.* 281:9552–9559.
- Lo, K.W., J.M. Kogoy, and K.K. Pfister. 2007a. The DYNLT3 light chain directly links cytoplasmic dynein to a spindle checkpoint protein, Bub3. *J. Biol. Chem.* 282:11205–11212.
- Lo, K.W., J.M. Kogoy, B.A. Rasoul, S.M. King, and K.K. Pfister. 2007b. Interaction of the DYNLT (TCTEX1/RP3) light chains and the intermediate chains reveals novel intersubunit regulation during assembly of the dynein complex. *J. Biol. Chem.* 282:36871–36878.
- Myers, K.R., K.W. Lo, R.J. Lye, J.M. Kogoy, V. Soura, M. Hafezparast, and K.K. Pfister. 2007. Intermediate chain subunit as a probe for cytoplasmic dynein function: Biochemical analyses and live cell imaging in PC12 cells. *J. Neurosci. Res.* 85:2640–2647.
- O'Rourke, S.M., M.D. Dorfman, J.C. Carter, and B. Bowerman. 2007. Dynein modifiers in *C. elegans*: light chains suppress conditional heavy chain mutants. *PLoS Genet.* 3:e128.
- Paschal, B.M., H.S. Shpetner, and R.B. Vallee. 1987. MAP 1C is a microtubule-activated ATPase which translocates microtubules in vitro and has dynein-like properties. *J. Cell Biol.* 105:1273–1282.
- Paschal, B.M., A. Mikami, K.K. Pfister, and R.B. Vallee. 1992. Homology of the 74-kD cytoplasmic dynein subunit with a flagellar dynein polypeptide suggests an intracellular targeting function. *J. Cell Biol.* 118:1133–1143.
- Pfister, K.K., M.W. Salata, J.F. Dillman III, E. Torre, and R.J. Lye. 1996a. Identification and developmental regulation of a neuron-specific subunit of cytoplasmic dynein. *Mol. Biol. Cell.* 7:331–343.
- Pfister, K.K., M.W. Salata, J.F. Dillman III, K.T. Vaughan, R.B. Vallee, E. Torre, and R.J. Lye. 1996b. Differential expression and phosphorylation of the 74-kDa intermediate chains of cytoplasmic dynein in cultured neurons and glia. *J. Biol. Chem.* 271:1687–1694.
- Pfister, K.K., E.M. Fisher, I.R. Gibbons, T.S. Hays, E.L. Holzbaur, J.R. McIntosh, M.E. Porter, T.A. Schroer, K.T. Vaughan, G.B. Witman, et al. 2005. Cytoplasmic dynein nomenclature. *J. Cell Biol.* 171:411–413.
- Pfister, K.K., P.R. Shah, H. Hummerich, A. Russ, J. Cotton, A.A. Annuar, S.M. King, and E.M. Fisher. 2006. Genetic analysis of the cytoplasmic dynein subunit families. *PLoS Genet.* 2:e1.
- Reilein, A.R., A.S. Serpinskaya, R.L. Karcher, D.L. Dujardin, R.B. Vallee, and V.I. Gelfand. 2003. Differential regulation of dynein-driven melanosome movement. *Biochem. Biophys. Res. Commun.* 309:652–658.
- Roy, S., M.J. Winton, M.M. Black, J.Q. Trojanowski, and V.M. Lee. 2007. Rapid and intermittent cotransport of slow component-b proteins. *J. Neurosci.* 27:3131–3138.
- Salata, M.W., J.F. Dillman III, R.J. Lye, and K.K. Pfister. 2001. Growth factor regulation of cytoplasmic dynein intermediate chain subunit expression preceding neurite extension. *J. Neurosci. Res.* 65:408–416.
- Sambrook, J., and D.W. Russell. 2001. *Molecular Cloning. A Laboratory Manual. Third Edition*. Cold Spring Harbor Laboratory Press, Cold Spring Harbor, NY. 16.14–16.18.
- Segal, R.A., A. Bhattacharyya, L.A. Rua, J.A. Alberta, R.M. Stephens, D.R. Kaplan, and C.D. Stiles. 1996. Differential utilization of Trk autophosphorylation sites. *J. Biol. Chem.* 271:20175–20181.
- Steegmaier, M., J. Klumperman, D.L. Foletti, J.S. Yoo, and R.H. Scheller. 1999. Vesicle-associated membrane protein 4 is implicated in trans-Golgi network vesicle trafficking. *Mol. Biol. Cell.* 10:1957–1972.
- Stepanova, T., J. Slemmer, C.C. Hoogenraad, G. Lansbergen, B. Dortland, C.I. De Zeeuw, F. Grosveld, G. van Cappellen, A. Akhmanova, and N. Galjart. 2003. Visualization of microtubule growth in cultured neurons via the use of EB3-GFP (end-binding protein 3-green fluorescent protein). *J. Neurosci.* 23:2655–2664.
- Susalka, S.J., and K.K. Pfister. 2000. Cytoplasmic dynein subunit heterogeneity: implications for axonal transport. *J. Neurocytol.* 29:819–829.
- Tai, A.W., J.Z. Chuang, C. Bode, U. Wolfmum, and C.H. Sung. 1999. Rhodopsin's carboxy-terminal cytoplasmic tail acts as a membrane receptor for cytoplasmic dynein by binding to the dynein light chain Tctex-1. *Cell.* 97:877–887.
- Tynan, S.H., A. Purohit, S.J. Doxsey, and R.B. Vallee. 2000. Light intermediate chain 1 defines a functional subfraction of cytoplasmic dynein which binds to pericentrin. *J. Biol. Chem.* 275:32763–32768.
- Vallee, R.B., J.C. Williams, D. Varma, and L.E. Barnhart. 2004. Dynein: An ancient motor protein involved in multiple modes of transport. *J. Neurobiol.* 58:189–200.
- Vaughan, K.T., and R.B. Vallee. 1995. Cytoplasmic dynein binds dynactin through a direct interaction between the intermediate chains and p150Glued. *J. Cell Biol.* 131:1507–1516.
- Watson, F.L., H.M. Heerssen, D.B. Moheban, M.Z. Lin, C.M. Sauvageot, A. Bhattacharyya, S.L. Pomeroy, and R.A. Segal. 1999. Rapid nuclear responses to target-derived neurotrophins require retrograde transport of ligand-receptor complex. *J. Neurosci.* 19:7889–7900.
- Wiedenmann, B., and W.W. Franke. 1985. Identification and localization of synaptophysin, an integral membrane glycoprotein of Mr 38,000 characteristic of presynaptic vesicles. *Cell.* 41:1017–1028.
- Winckler, B., P. Forscher, and I. Mellman. 1999. A diffusion barrier maintains distribution of membrane proteins in polarized neurons. *Nature.* 397:698–701.
- Yano, H., F.S. Lee, H. Kong, J. Chuang, J. Arevalo, P. Perez, C. Sung, and M.V. Chao. 2001. Association of Trk neurotrophin receptors with components of the cytoplasmic dynein motor. *J. Neurosci.* 21:RC125.
- Ye, H., R. Kuruvilla, L.S. Zweifel, and D.D. Ginty. 2003. Evidence in support of signaling endosome-based retrograde survival of sympathetic neurons. *Neuron.* 39:57–68.
- Zhang, H., D.J. Webb, H. Asmussen, and A.F. Horwitz. 2003. Synapse formation is regulated by the signaling adaptor GIT1. *J. Cell Biol.* 161:131–142.